Temporal resolution of a pre-maximum halt in a classical nova: V5589 Sgr observed with *STEREO* HI-1B

S. P. S. Eyres,[1][*] D. Bewsher,[1] Y. Hillman,[2] D. L. Holdsworth,[1] M. T. Rushton,[1,3] D. Bresnahan,[1] A. Evans[4] and P. Mróz[5]

[1]*Jeremiah Horrocks Institute, University of Central Lancashire, Preston PR1 2HE, UK*
[2]*Department of Geosciences, Raymond and Beverly Sackler Faculty of Exact Sciences, Tel-Aviv University, Tel-Aviv 69978, Israel*
[3]*Astronomical Institute of the Romanian Academy, Str. Cutitul de Argint 5, 040557 Bucuresti, Romania*
[4]*Astrophysics Group, Keele University, Keele, Staffordshire ST5 5BG, UK*
[5]*Warsaw University Observatory, Al. Ujazdowskie 4, PL-00-478 Warszawa, Poland*

ABSTRACT

Classical novae show a rapid rise in optical brightness over a few hours. Until recently the rise phase, particularly the phenomenon of a pre-maximum halt, was observed sporadically. Solar observation satellites observing coronal mass ejections enable us to observe the pre-maximum phase in unprecedented temporal resolution. We present observations of V5589 Sgr with *STEREO* HI-1B at a cadence of 40 min, the highest to date. We temporally resolve a pre-maximum halt for the first time, with two examples each rising over 40 min then declining within 80 min. Comparison with a grid of outburst models suggests that this double peak, and the overall rise time-scale, is consistent with a white dwarf mass, central temperature and accretion rate close to $1.0\,M_\odot$, 5×10^7 K and $10^{-10}\,M_\odot\,yr^{-1}$, respectively. The modelling formally predicts mass-loss onset at JD 245 6038.2391 $\pm$ 0.0139, 12 h before the optical maximum. The model assumes a main-sequence donor. Observational evidence is for a sub-giant companion, meaning that the accretion rate is underestimated. Post-maximum, we see erratic variations commonly associated with much slower novae. Estimating the decline rate is difficult, but we place the time to decline two magnitudes as $2.1 < t_2(\mathrm{d}) < 3.9$, making V5589 Sgr a 'very fast' nova. The brightest point defines 'day 0' as JD 245 6038.8224 $\pm$ 0.0139, although at this high cadence the meaning of the observed maximum becomes difficult to define. We suggest that such erratic variability normally goes undetected in faster novae due to the low cadence of typical observations, implying that erratic behaviour is not necessarily related to the rate of decline.

Key words: stars: individual: V5589 Sgr – novae, cataclysmic variables.

1 INTRODUCTION

Classical novae are interacting binary stars, in which a white dwarf (WD) accretes matter from a (usually) main-sequence-like companion, generally in a close orbit with a period of a few hours to days. This results in a build-up of material on the WD surface, leading to thermonuclear runaways that cause an outburst, at ultraviolet (UV), optical and infrared (IR) wavelengths in a few hours, and the ejection of around 10^{-5}–$10^{-4}\,M_\odot$ of matter at velocities of a few 100 to a few $1000\,km\,s^{-1}$ (Warner 2008). Decline then follows over the course of weeks or months, with the time to drop 2 or 3 mag from maximum related to the absolute magnitude through the maximum-magnitude-rate-of-decline relationship (MMRD; Downes & Duerbeck 2000), for both Galactic

and extra-galactic populations (Darnley et al. 2006). Slower novae often show erratic variations and remain bright for longer times than is consistent for the MMRD, when considered in light of independent distance measurements. The relationship is also not useful for novae that decline most rapidly, as the absolute magnitude becomes insensitive to decline time (e.g. Capaccioli et al. 1990).

Recently observations and theoretical developments have established that prior to optical maximum X-ray and even gamma-ray emission is seen (Ackermann et al. 2014). Due to the rate of ascent, the *pre-maximum* optical light curve has been only rarely observed, and at cadences of 1–2 data points per day. Some show a pre-maximum halt (PMH) that had not been subjected to theoretical modelling.

Hounsell et al. (2010) presented four light curves taken with the *Solar Mass Ejection Imager* down to time resolutions of 80 min, showing the PMH to be ubiquitous in their sample. Further analysis of SMEI light-curves of novae was presented by Hounsell et al.

(2016), with a catalogue of 14 systems. They derived peak time, maximum magnitude and an estimate of the rate of decline for all systems, and tentatively detected PMHs in two of their sample. Hillman et al. (2014) have demonstrated that the form of these halts varies with the gross parameters of WD mass, WD central temperature and the accretion rate from the companion.

Here, we present data from the *Solar TErrestrial RElations Observatory (STEREO)* HI-1B camera for V5589 Sgr, following the outburst from the initial rise, through the optical peak to the point where it fades below detectability for this instrument. The cadence is around 40 min, making these the highest time resolution observation of this phase to date. We discuss the rise phase, including the PMHs, in the context of the models of Hillman et al. (2014). We also contrast the post-maximum behaviour with much slower classical novae (CNe), and suggest that the empirical split in this behaviour between slow and fast novae is in part a function of the typical one day sampling of the light curves.

2 V5589 SGR

V5589 Sgr (Nova Sgr 2012, PNV J17452791–2305213, coordinates J2000 17 45 28.03 −23 05 22.7) was discovered on 2012 April 21.0112 UT (Sokolovsky et al. 2012) at $V \sim 9.6$, rising to a reported maximum of $V = 8.8$ (Korotkiy et al. 2012) by 2012 April 21.654 UT (CBAT 2015). Pre-discovery images detected the outburst on 2012 April 20.8403 UT down to $V = 10.2$ (CBAT 2015).

Early spectroscopy indicated high-velocity ejecta in this nova, with linewidths (full width at half-maximum) of 5600 (Korotkiy et al. 2012) to 6500 km s^{-1} (Esipov, Sokolovsky & Korotkiy 2012). Observations in X-ray (Sokolovsky et al. 2012; Nelson et al. 2012a) and radio (Nelson et al. 2012a) wavelengths shortly after optical peak showed non-detections, and suggested no shocked component in the expanding ejecta at this early stage of the decline.

Swift UVOT detected the object on 2012 April 25.7 at a UVM2 brightness of 13.71 ± 0.09 mag, fading rapidly from 13.8 to 13.5 over a 5975 s observation (Nelson et al. 2012b). By 2012 May 10, hard X-ray emission was present, consistent with a column density of $N(H) = (3 \pm 1) \times 10^{21}$ cm^{-2} and a plasma temperature of at least 2.7×10^8 K; the UVM2 brightness was 16.0 ± 0.2 mag by this date (Nelson et al. 2012b). Weston et al. (2016) argue that the radio and X-ray characteristics are consistent with high-speed, low-mass ejecta that accelerates over the first few weeks after outburst.

The nova has been observed by the OGLE survey since 2010 (Mróz et al. 2015). In the quiescent light curve, they found eclipses with a period of 1.59230(5) d, which they interpret as the orbital period. Such a relatively long orbital period suggests that the secondary is a subgiant. If the secondary fills its Roche lobe, the orbital period can be used to estimate the radius of the secondary (see e.g. King 1989). Using equation (2.3.10) of King, we find that the secondary radius $R_2/R_\odot \sim 0.11 P_{hr} \sim 4.2\,R_\odot$, confirming that the secondary is evolved. The last pre-eruption image was taken on 2012 April 20.3728 UT at $I = 16.90$. These authors also note that with this longer period, the companion is likely to be a subgiant. Weston et al. (2016) come to the same conclusion.

3 OBSERVATIONS

The *STEREO* consists of two nearly identical spacecraft, in heliocentric orbits, one ahead of the Earth (*STEREO-A*) and the other behind the Earth (*STEREO-B*) (Kaiser et al. 2008). The twin spacecraft were launched on 2006 October 26, and the separation between

each spacecraft and the Earth has increased by approximately 22° per year since achieving heliocentric orbits.

The Sun Earth Connection Coronal and Heliospheric Investigation (SECCHI) instrument suite (Howard et al. 2008) on *STEREO* includes the heliospheric imagers (HI-1 and HI-2). The HI instruments have been used to observe a variety of variable stars, including the classical nova V5583 Sgr (Holdsworth et al. 2014), and long-period variables (Wraight et al. 2012).

Data from the HI-1 instrument on *STEREO-B* (HI-1B) are used in this paper. HI-1B has a field of view of 20°, which extends from ∼4° to 24° elongation, with a pixel size of ∼70 arcsec (Eyles et al. 2009). The *STEREO* HI-1B instrument's main passband covers the range from 600 to 750 nm, but also has contributions at 300–450 nm and from 900 to 1100 nm (see fig. 6 of Bewsher et al. 2010).

The HI-1B images consist of 30 exposures of 40 s each, with a summed image cadence of 40 min (Eyles et al. 2009). Each exposure is scrubbed of cosmic-ray hits prior to summing (Howard et al. 2008). The summed images constitute the L0.5 FITS files, which are available for download from several websites, including the UK Solar System Data Centre (UKSSDC[1]).

The L0.5 data have been prepared with the SSWIDL procedure, SECCHI_PREP. This routine applies the shutterless correction to the data, the large-scale flat-field determined by Bewsher et al. (2010), and the pointing and optical parameter calibration of Brown, Bewsher & Eyles (2009). It also identifies missing blocks and saturated pixels, filling these pixels with NaN values.

As discussed in Bewsher et al. (2010), the point spread function of the HI-1B instrument is well approximated with a Gaussian profile, and the aperture size of 3.1 pixels suggested by Bewsher et al. (2010) is used to extract the nova light curve from the data using aperture photometry. The solar F-corona is the dominant source in the HI-1B data, and is removed using a daily running background.

To extract the light curve presented in this paper, each HI image is processed with SECCHI_PREP, and the position of the nova determined using the pointing information given in the header of the FITS file. Aperture photometry is performed on this position, and the number of counts (DN s^{-1}) recorded. This process is repeated for every HI image from 2012 April 18 to May 7, where the nova crosses the CCD of the instrument. The counts recorded are then converted into a magnitude using the following equation:

$$M_{\mathrm{HI}} = -2.5 \log \left(\frac{I_{\mathrm{tot}}}{\mu F} \right), \tag{1}$$

where M_{HI} is the HI magnitude, I_{tot} is the recorded counts, μ is a calibration conversion factor and F is the flux of Vega (Bewsher et al. 2010), the zero-point of the magnitude scale. The error on μF, σ_{F}, is estimated to be of the order of 5 per cent:

$$\frac{\sigma_{\mathrm{F}}}{\mu F} = 0.05. \tag{2}$$

It is assumed that the uncertainties on I_{tot}, σ_I, are Poisson counting statistics, and the conversion from DN (units of I_{tot}) to photoelectrons is 1 DN = 15 photoelectrons (Eyles et al. 2009); therefore

$$\sigma_I = \sqrt{\frac{I_{\mathrm{tot}}}{15}}. \tag{3}$$

The uncertainty on the magnitude measurement is then given by

$$\sigma_{M_{\mathrm{HI}}} = \left| \frac{-2.5}{\ln(10)} \sqrt{\left(\frac{\sigma_I}{I_{\mathrm{tot}}} \right)^2 + \left(\frac{\sigma_{\mathrm{F}}}{\mu F} \right)^2} \right| \tag{4}$$
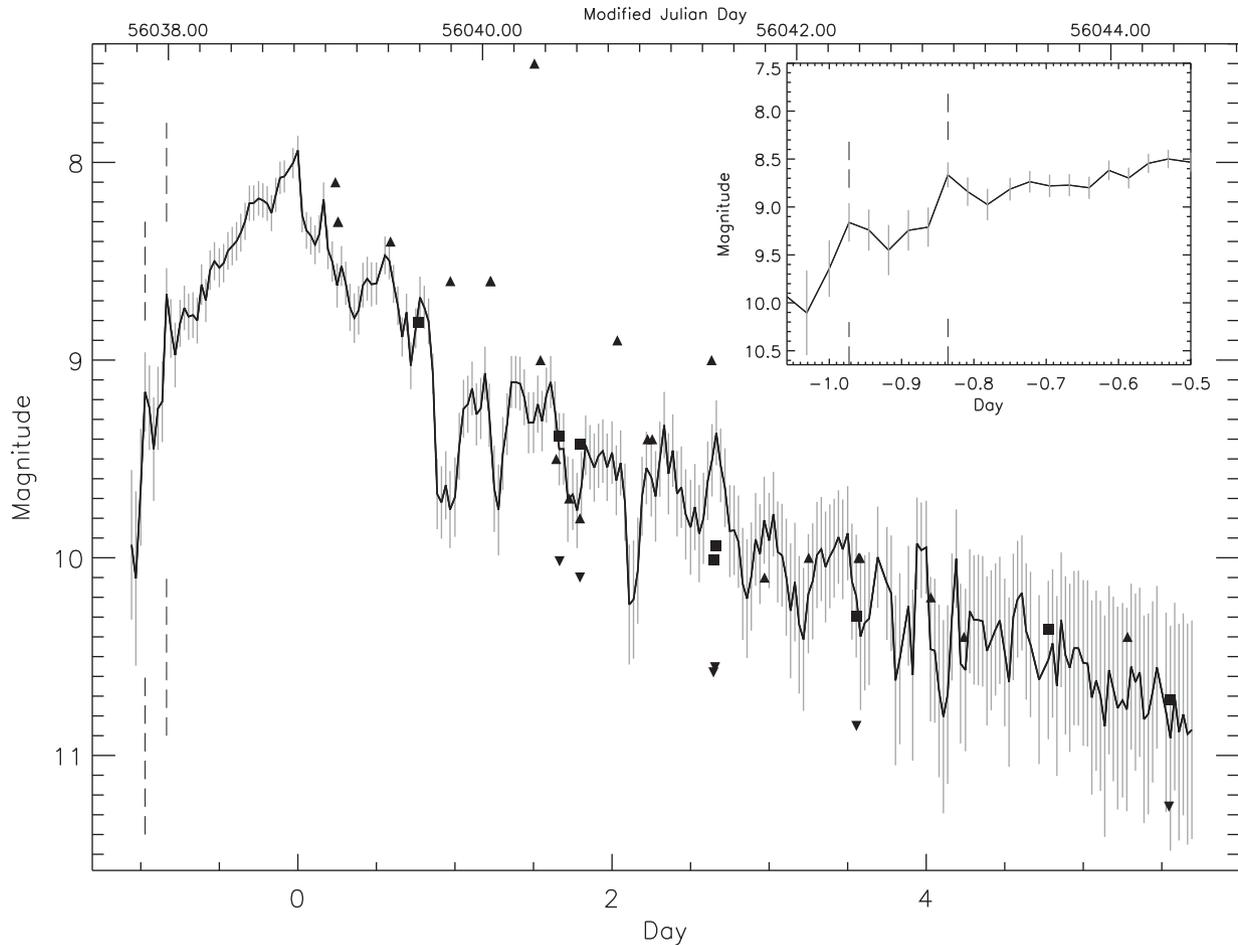
[1] http://www.ukssdc.ac.uk/

Figure 1. *STEREO* HI-1B data with error bars, plus AAVSO visual estimates (triangles), V (squares) and B (inverted triangles) included for comparison; offset by 1 mag upwards for clarity. *STEREO* is approximately *R* band, for which data are available in AAVSO only after JD 245 6051 (MJD 56051.5), about 6 d after the end of this data run. Vertical dashed lines mark the PMHs described in the text. The inset zooms in on the ∼14 h period around the PMHs.

$$= \left| \frac{-2.5}{\ln(10)} \sqrt{\left(\frac{\sqrt{\frac{I_{tot}}{15}}}{I_{tot}}\right)^2 + (0.05)^2} \right|. \quad (5)$$

This value was calculated on a point-by-point basis and is included in Fig. 1 as error bars. The error due to the background subtraction has not been included in the errors on the light curve. However, it is estimated that the error due to the background subtraction is of the order of 10 per cent of the calculated error for a handful of points, and less than 5 per cent for the majority of points. This is due to the background subtraction being calculated using the average over a days worth of observations, leading to comparatively small uncertainties.

In the following, we use the 40 min cadence of the data as the basis for uncertainties in any dates or intervals in time. This translates to ±0.0139 d, with the third decimal place being conservative, given that observations are made at this cadence to within a few seconds.

4 RESULTS

The light curve of V5589 Sgr is presented in Fig. 1. We see the rise to maximum, and then a rather erratic decline. We also overlay American Association of Variable Star Observers (AAVSO) B, V and visual estimate data for comparison. Uncertainties in AAVSO visual estimates are estimated as 0.1 mag, although this varies with location and experience of the contributing observers. We can see that while the *STEREO* and AAVSO data are consistent, the latter has a much lower cadence and relies primarily on visual estimates.

The time of maximum is a key characteristic determined for previous novae, and often used to refer to subsequent development, with the brightest point labelled 'day 0'. As the decline time from peak is used to determine the speed class of CNe (Payne-Gaposhkin 1957; Duerbeck 2008), which, in turn, correlates with the energetics of the event, it is useful to identify this point. There is one brightest point in the *STEREO* data, albeit less than 1σ above adjacent points. This point is at JD 245 6038.8224 ± 0.0139, and can be taken as the peak magnitude.

Determining the time to decline by two magnitudes, t_2, and hence the speed class, is somewhat more uncertain. The brightness at peak is 7.94 ± 0.09, and the brightness drops below 9.94 for the first time after JD 245 6040.9057 ± 0.0139 but recovers 2 h later. The last time it is brighter than this is the point at JD 245 6042.3224. The average magnitude binned over 18 points (12 h interval) reaches this level in the bin centred on JD 245 6041.7668. These give a t_2 time of between 2.1 and 3.9 d, placing the nova firmly in the 'very fast' class. The *STEREO* passband incorporated more red light than the *B* or *V* bands, where t_2 is usually determined. None the less, the values are well within the 'very fast' range, and there is an expectation that this object will be in the upper range for intrinsic luminosity and

velocity of the ejecta of the nova events. This is consistent with the identification of a high-speed shock by Weston et al. (2016).

4.1 Pre-maximum halts

A key finding of our work is the presence in the rise phase of deviations from a monotonic increase that are consistent with PMHs seen in other classical novae. For V5589 Sgr, we have identified two short deviations – peaking at JD 245 6037.8502 $\pm$ 0.0139 and JD 245 6037.9891 $\pm$ 0.0139 – with this phenomenon. From Fig. 1, we can see that the rise to peak occurs between one point and the next (i.e. within 40 min), with the decline over three points (i.e. over 80 min), both with the same shape within the uncertainties. As the PMHs appear, V5589 Sgr moves between pixels 80 and 110 along the 540th row of the CCD, so the nova is well away from the edge of the 1024 $\times$ 1024 pixel detector.

The initial rise reflects a change of more than 3σ point-to-point as a PMH starts (uncertainties decline with increasing brightness). The PMH decline is to a level within 2σ of the pre-rise magnitude. Modelling by Hillman et al. (2014) suggests that PMHs are often short-lived excursions above the general upward trend of the rise. We explore this by taking linear interpolations between the 'before' and 'after' points for both features. These are found to follow a line consistent with the subsequent rise. Thus, the two peaks are consistent with being such excursions from the general upward trend, rather than being defined by dips that interrupt the rise. The combination of the change relative to the uncertainties and the deviation from what one would expect from backward extrapolation of the rise allows us to be confident that they can be reasonably described as PMHs, as modelled by Hillman et al. (2014).

5 DISCUSSION

We discuss the PMHs during the rise phase, and then the behaviour following the optical peak.

5.1 Double PMH

During the rise to maximum (Fig. 1), we see two very similar features that represent departures from the smooth, monotonic rise normally considered to be the usual behaviour for CNe before the optical peak. We have interpreted these as the sometimes-observed PMHs. When taken in combination with those seen by Hounsell et al. (2010), we can conclude that these events are common, and have been generally missed in historical observations.

In Fig. 2, we compare a model from the grid of Hillman et al. (2014) with the *STEREO* data. We have chosen parameters that give the best qualitative agreement with the data. We have not attempted to fit the parameters to the data, but instead we offer this as support that the general development of the PMHs during the rise is understood. The model plot shows the relevant time period from fig. 4, Panel 4, plot 100.50.10 of Hillman et al. (2014). The model starts from well before the span of the data, and to assess the similarity, we have simply aligned the peak of the second halt. By inspection, we can then see that the duration, magnitude and interval between the halts are consistent between the model and the data. The PMHs occur in the model at the point when convection ceases to be efficient near the surface causing a reduction in the energy flux. The opacity then decreases allowing radiation to become the dominant energy transfer mechanism and reverse the dip. This starts to drive mass-loss.
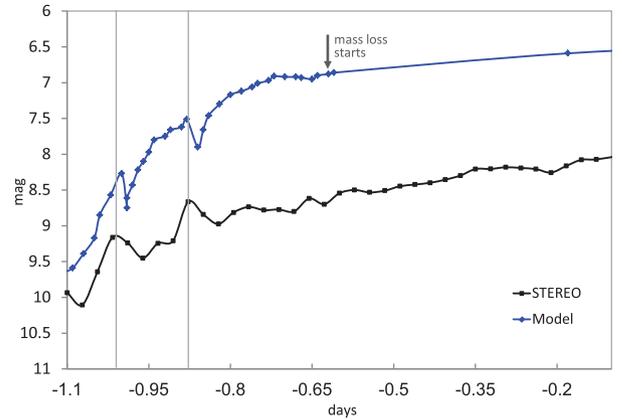

Figure 2. Comparison of data (lower line) and model (upper line) for the parameters giving the closest match to the pre-maximum behaviour (WD mass 1.0 $M_\odot$, central temperature 5 $\times$ 10^7 K and mass accretion rate 10^{-10} $M_\odot$ yr^{-1}). The time axis is relative to day 0 at JD 245 6038.8224.

The model agrees less well with the behaviour of V5589 Sgr once convection ceases to dominate evolution around the PMHs. None the less, we have constrained the onset of mass-loss to occur between the peak of the first PMH and the maximum of the optical light (i.e. between JD 245 6037.8502 and JD 245 6038.8224), with the model formally giving this as JD 245 6038.2391. The modelling assumes a main-sequence donor star. While the subgiant donor would have a lower H abundance, this simply means the accretion rate derived from the model is an underestimate of the true rate. An optical spectrum in quiescence would be valuable to confirm the nature of the secondary.

5.2 Post-maximum erratic decline

There are a number of excursions visible in Fig. 1 significantly above or below the mean magnitude during the decline after day 0. We consider if any of this structure is consistent with periodicity. We also examine how significant the excursions are, given the overall scatter in the data.

An orbital period of 1.592 30 d determined by Mróz et al. (2015) is based on the ephemeris of HJD = 2455000.724 $\pm$ 0.015 + (1.59230 $\pm$ 0.00005) $\times$ E for the eclipses.

To test for periodicities in the decline phase, we excluded data obtained before day 0 and perform a discrete Fourier transform (FT) on the remaining data using the PERIOD04 software of Lenz & Breger (2005). After fitting and removing the slope of the decline, we search for significant periods in the de-trended data. Given the quality of the observations, we relax the 'standard' signal-to-noise ratio limit of 4 (e.g. Koen 2010) to 3 to determine if a peak in the FT is significant; however, we find no peaks in the FT above this limit. Furthermore, there is no evidence in our data of the orbital period determined by Mróz et al. (2015).

This is consistent with post-outburst Optical Gravitational Lensing Experiment (OGLE) observations showing that eclipses do not start occurring again until HJD = 2456062.82544 or possibly as late as HJD = 2456076.92252. Prior to this, the entire binary must be within the photosphere of the nova ejecta, and so must be larger than the orbital radius of $\sim$7.2 $R_\odot$ $\times$ ($M/2$ $M_\odot$)$^{1/3}$ for a system mass of M.

While there are a number of variations in the decline phase, none is consistently separated by this interval, or a multiple thereof.

In addition, a simple polynomial fit to the decline suggests that only the minima centred around MJD 56039.7668, 56040.1002 and 56040.9335 are consistent with anything other than the overall level of fluctuations seen. None of these are separated by the period in Mróz et al. (2015). Thus, whatever the origin of these dips, neither eclipses nor orbital modulation appears to explain them.

The speed class appears to be related both to the luminosity of the nova at the peak and to the kinetic energy of the ejecta, with both being higher for faster novae. Much less consistently, more slowly declining examples often show erratic brightening and dimming after the initial rise, presenting multiple false maxima and making the determination of the peak, and hence the decline rate, difficult. Evans et al. (2003) discuss V723 Cas as an example, and suggest that these 'flare-like' features might be due to interactions within the ejecta or mass transfer bursts from the companion, as proposed by Chochol, O'Brien & Bode (2000). By contrast, erratic behaviour is not generally seen in fast examples of CNe, where the rise and fall is seen to be smooth. However, the vast majority of ground-based light curves are made up of a number of observations every night, with a considerable variation in the consistency of observations, and are mainly visual estimates. The data presented here provide unprecedented stability and point-to-point reliability at a regular 40 min cadence.

Hounsell et al. (2010) found some erratic behaviour early on in V1280 Sco and to a lesser extent in KT Eri, the second also being very fast. As noted in their section 4, the decline time and the form of the PMHs do not seem to have any correlation; V5589 Sgr shows a different form again, even though the initial decline rate was similar to that of KT Eri. We suggest that the association of erratic brightness variations near peak with slower novae is a feature of the poor cadence of most light-curve data to date. It is clearly a feature of some examples of fast novae, but at this point we do not have enough examples to judge if it is less common than in slower novae. Hounsell et al. (2016) showed further examples of non-smooth declines from maximum in many of their novae light curves, however due to the limiting magnitude and contamination the presence of erratic variations may not be astrophysical.

In fact, once we start to record the early light curve of novae at the cadence achieved here, the definition of 'day 0' needs to be revisited. An alternative approach to determining the peak in Fig. 1 is to treat all fluctuations from a smooth rise and decline as anomalous. In this case, some form of fit to the overall rise and decline might be used to give an estimate of the peak that is derived in a manner consistent with those for novae with only low-cadence data. A second-order polynomial fit through the peak has a maximum of 8.16 ± 0.10 mag, at 56038.68, or 160 min earlier than the absolute brightest measurement used to define 'day 0' in Section 4. Thus, at this high cadence, where we see fluctuations on time-scales of a few hours, the relevance of optical maximum and hence 'day 0' starts to become problematic. However, as *STEREO* and other facilities allow us to examine an increasing number of fast novae in this detail, we may be able to reassess the speed class concept.

6 CONCLUSIONS

We have collected an optical light curve of the fast classical nova V5589 Sgr at a time resolution of 40 min, the best for any nova to date. These data show the rise to maximum with pre-maximum halts, and the subsequent somewhat erratic decline, in greater detail than seen before. We find that the halts are consistent with a binary model having a WD of mass $1.0 \, M_\odot$, central temperature 5×10^7 K and

mass accretion rate $10^{-10} \, M_\odot \, yr^{-1}$. As the donor star is a subgiant, the last of these is likely an underestimate. The model shows that the PMHs are pre-cursors to the onset of mass-loss and formally predicts this as starting at JD 245 6038.2391 $\pm$ 0.0139 for V5589 Sgr.

We suggest that the erratic decline behaviour, a common characteristic of slow novae, is missed in previous observations of some faster examples by the typical daily observations. Our work, and that of Hounsell et al. (2010), demonstrate that some fast novae also demonstrate erratic behaviour close to optical peak. This is not understood or well modelled at this time. We also find that at such high cadence, the common identification of the peak as 'day 0' becomes increasingly difficult and possibly misleading.

STEREO-A continues to operate and we will retrieve data of further CNe that are serendipitously bright as they cross one or more of the four camera apertures. This will allow us to investigate the prevalence and nature of PMHs, and any erratic behaviour close to optical maximum.

REFERENCES

Ackermann M. et al., 2014, Science, 345, 554
Bewsher D., Brown D. S., Eyles C. J., Kellett B. J., White G. J., Swinyard B., 2010, Sol. Phys., 264, 433
Brown D. S., Bewsher D., Eyles C. J., 2009, Sol. Phys., 254, 185
Capaccioli M., della Valle M., D'Onofrio M., Rosino L., 1990, ApJ, 360, 63
CBAT, 2015, 'Transient Object Followup Reports' PNV J17452791-2305213. Available at: http://www.cbat.eps.harvard.edu/unconf/followups/J17452791-2305213.html
Chochol D., O'Brien T. J., Bode M. F., 2000, New Astron. Rev., 44, P61
Darnley M. J. et al., 2006, MNRAS, 369, 257
Downes R. A., Duerbeck H. W., 2000, AJ, 120, 2007
Duerbeck H. W., 2008, in Bode M. F., Evans A., eds, Classical Novae. Cambridge Univ. Press, Cambridge, p. 1
Esipov V. F., Sokolovsky K. V., Korotkiy S., 2012, The Astronomer's Telegram, 4094
Evans A. et al., 2003, AJ, 126, 1981
Eyles C. J. et al., 2009, Sol. Phys., 254, 387
Hillman Y., Prialnik D., Kovetz A., Shara M. M., Neill J. D., 2014, MNRAS, 437, 1962
Holdsworth D. L., Rushton M. T., Bewsher D., Walter F. M., Eyres S. P. S., Hounsell R., Darnley M. J., 2014, MNRAS, 438, 3483
Hounsell R. et al., 2010, ApJ, 724, 480
Hounsell R. et al., 2016, ApJ, 820, 104

Howard R. A. et al., 2008, Space Sci. Rev., 136, 67

Kaiser. M. L., Kucera T. A., Davila J. M., St. Cyr O. C., Guhathakurta M., Christian E., 2008, Space Sci. Rev., 136, 5

King A. R., 1989, in Bode M. F., Evans A., eds, Classical Novae. Wiley, Chichester, p. 16

Koen C., 2010, Ap&SS, 329, 267

Korotkiy S. et al., 2012, Cent. Bur. Electron. Telegrams, 3089, 1

Lenz P., Breger M., 2005, Commun. Asteroseismol., 146, 53

Mróz P. et al., 2015, ApJS, 219, 26

Nelson T., Mukai K., Sokoloski J., Chomiuk L., Rupen M., Mioduszewski A., 2012a, The Astronomer's Telegram, 4088

Nelson T., Mukai K., Sokoloski J., Chomiuk L., Rupen M., Mioduszewski A., 2012b, The Astronomer's Telegram, 4110

Payne-Gaposhki C., 1957, The Galactic Novae. North-Holland, Amsterdam

Sokolovsky K., Korotkiy S., Elenin L., Molotov I., 2012, The Astronomer's Telegram, 4061

Warner B., 2008, in Bode M. F., Evans A., eds, Classical Novae. Cambridge Univ. Press, Cambridge, p. 16

Weston J. H. S. et al., 2016, MNRAS, 460, 2687

Wraight K. T., Bewsher D., White Glenn J., Nowotny W., Norton A. J., Paladini C., 2012, MNRAS, 426, 816

This paper has been typeset from a TEX/LATEX file prepared by the author.